Biophysical Chemistry 21 (1985) 81–89
Elsevier

BPC 00889

THEORY OF COUNTERION ELECTROPHORESIS

GUIDELINES FOR DETERMINATION OF LIGAND-BINDING PARAMETERS

John R. CANN and Nancy H. FINK *

Department of Biochemistry/Biophysics/Genetics, University of Colorado Health Sciences Center, 4200 E. 9th Avenue, Denver, CO 80262, U.S.A.

Received 7th March 1984
Accepted 22nd May 1984

Key words: Counterion electrophoresis; Counterion electrophoresis theory; Ligand-binding parameter determination; Steady-state binding parameter; Thermodynamic binding parameter

A theory is formulated to provide guidelines for the quantitative interpretation of steady-state counterion electrophoretic patterns (T.-H. Ueng and F. Bronner, Arch. Biochem. Biophys. 197 (1979) 205) in terms of intrinsic ligand-binding constant and number of binding sites on the protein molecule. Briefly, the prescribed procedure calls for extrapolation of the steady-state binding constant to infinite dilution of protein to obtain a quantity which is the product of a readily evaluated kinetic factor and the intrinsic binding constant. On the other hand, extrapolation of the steady-state number of binding sites to infinite dilution can probably be dispensed with if determined at a reasonably low protein concentration.

1. Introduction

The method of counterion electrophoresis was originally developed by Ueng and Bronner [1] to identify calcium-binding proteins in conventional polyacrylamide gel disc electrophoretic patterns and to quantitate binding in terms of intrinsic association constant and number of binding sites on the protein molecule. The procedure is as follows: Labeled calcium ($^{45}CaCl_2$) is added to the buffer in the lower (anode) chamber reservoir and a sample of negatively charged protein is applied to the polyacrylamide gel in the cathode chamber reservoir. Under the influence of the applied electric field the zone(s) of protein migrates down the gel column, and calcium is driven into and up the column where it complexes with the protein. The system eventually reaches a steady state in which calcium is uniformly distributed (apparent baseline) along the lengths of column in front of and behind the advancing zone of protein and its complexes with calcium, the equilibrium composition of the zone being determined by the local concentration of unbound calcium. The gel is sliced, and the concentration of calcium in the slices determined by radioactive counting. What we shall designate as the steady-state amount of calcium bound is determined by subtracting the apparent baseline concentration from the total concentration of calcium in the protein zone. By varying the concentration of calcium added to the anode chamber reservoir, a double-reciprocal plot of steady-state amount bound against apparent baseline concentration is constructed, and steady-state values of the binding constant and the maximum amount bound determined therefrom.

While this procedure was developed to study calcium binding, it can obviously be applied to other cationic ligands and to anionic ones as well,

* Present address: Department of Biochemistry, Willard Hall, Kansas State University, Manhattan, KA 66506, U.S.A.

whether the protein is negatively or positively charged. In general, however, the steady-state binding constant determined as described above is not a thermodynamic equilibrium constant, because the local concentration of unbound ligand in the protein zone is not the same as the apparent baseline concentration [1]. Accordingly, we have formulated a theory of counterion electrophoresis which provides guidelines for determination of this fundamental quantity.

2. Theory

The theory consists of two parts: (1) The combined analytical application of the law of conservation of mass and the ligand-binding isotherm to the counterion electrophoretic procedure described above; and (2) numerical calculation of counterion electrophoretic patterns. Both parts treat the steady state eventually reached in the electrophoresis column as a result of the continual flux of ligand through the column under the influence of the applied electric field, and are silent with respect to the approach to the steady state.

2.1. Analytical deductions

Let us start by recalling that the ligand, $\mathscr{L}$, interacts with the protein, $\mathscr{P}$, to form a number of complexes, $\mathscr{P}\mathscr{L},\ldots,\mathscr{P}\mathscr{L}_i,\ldots,\mathscr{P}\mathscr{L}_n$, where n is the maximum number of binding sites on the protein molecule. Formation of the successive complexes may be represented by the equilibria [2,3]

$$\begin{aligned}
&\mathscr{P}+\mathscr{L}\rightleftharpoons\mathscr{P}\mathscr{L}\\
&\vdots\\
&\mathscr{P}\mathscr{L}_{i-1}+\mathscr{L}\rightleftharpoons\mathscr{P}\mathscr{L}_i\\
&\vdots\\
&\mathscr{P}\mathscr{L}_{n-1}+\mathscr{L}\rightleftharpoons\mathscr{P}\mathscr{L}_n
\end{aligned}\qquad(1)$$

It is assumed that the rates of complex formation and dissociation are sufficiently fast that local chemical equilibrium prevails at every instant of electrophoresis. In general, the electrophoretic velocities of the complexes, $V_{\mathscr{P}\mathscr{L}_i}$, will differ from the uncomplexed protein, $V_{\mathscr{P}}$, in which case the zone of protein will migrate with the constituent velocity of the protein in the equilibrium mixture of $\mathscr{P}$ and its complexes, $\bar{V}_{\mathscr{P}}$. The constituent molar concentration of the protein is designated by $\bar{C}_{\mathscr{P}}$; concentration of protein-ligand complexes, $C_{\mathscr{P}\mathscr{L}_i}$; electrophoretic velocity of unbound ligand, $V_{\mathscr{L}}$; and concentration of unbound ligand, $C_{\mathscr{L}}$.

Consider, with the aid of fig. 1, the steady-state flux of constituent ligand across two transverse, moving planes perpendicular to the electrophoresis column. The planes, designated α and β, move with the constituent velocity of the protein, the α-plane migrating down the length of column in front of the advancing zone of protein and the β-plane moving coincident with the center of mass of the protein. Concentrations at the instantaneous position of the planes are denoted by superscript α or β. Conservation of mass requires that

$$\begin{aligned}
\left(V_{\mathscr{L}}-\bar{V}_{\mathscr{P}}\right)C^{\alpha}_{\mathscr{L}} &= \left(V_{\mathscr{L}}-\bar{V}_{\mathscr{P}}\right)C^{\beta}_{\mathscr{L}}\\
&\quad+\sum_{i=1}^{n} i\left(V_{\mathscr{P}\mathscr{L}_i}-\bar{V}_{\mathscr{P}}\right)C^{\beta}_{\mathscr{P}\mathscr{L}_i},
\end{aligned}\qquad(2)$$

which, upon division by $(V_{\mathscr{L}}-\bar{V}_{\mathscr{P}})$ followed by rearrangement, gives

$$C^{\beta}_{\mathscr{L}}=C^{\alpha}_{\mathscr{L}}-\sum_{i=1}^{n} i\frac{\left(V_{\mathscr{P}\mathscr{L}_i}-\bar{V}_{\mathscr{P}}\right)}{\left(V_{\mathscr{L}}-\bar{V}_{\mathscr{P}}\right)}C^{\beta}_{\mathscr{P}\mathscr{L}_i}.\qquad(3)$$

It can be seen by inspection that for interaction of a negatively charged protein with a cationic ligand, $C^{\beta}_{\mathscr{L}}<C^{\alpha}_{\mathscr{L}}$ so that the experimental value of the

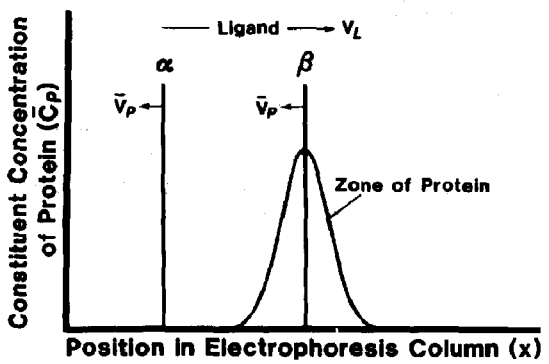

Fig. 1. Diagrammatic representation of counterion electrophoresis.

steady-state amount bound would be smaller than the actual amount bound. Consequently, the steady-state binding constant would be smaller than the thermodynamic equilibrium constant; vice versa for positively charged protein and anionic ligand. Moreover, the higher the protein concentration, the larger is the effect. Elaboration of these concepts is the crux of our investigation.

We proceed from the definition of the steady-state number of moles of $\mathscr{L}$ bound per mole of total protein, ν_{ss}: For either an infinitely sharp zone of protein or a zone broadened by diffusion and reaction and in which $C_{\mathscr{P}\mathscr{L}_i}$, $\bar{C}_{\mathscr{P}}$ and $(C_{\mathscr{L}} - C^{\alpha}_{\mathscr{L}})$ are distributed with the same moments about the center of mass of the protein

$$\nu_{ss} = \frac{\sum_{i=0}^{n} iC^{\beta}_{\mathscr{P}\mathscr{L}_i} + C^{\beta}_{\mathscr{L}} - C^{\alpha}_{\mathscr{L}}}{\sum_{i=0}^{n} C^{\beta}_{\mathscr{P}\mathscr{L}_i}} = \nu^{\beta} + \frac{C^{\beta}_{\mathscr{L}} - C^{\alpha}_{\mathscr{L}}}{C^{\beta}_{\mathscr{P}}} \tag{4}$$

where ν^{β} is the actual moles of $\mathscr{L}$ bound per mole of protein at position β. Let us consider statistical binding to n equivalent sites with intrinsic binding constant k, in which case the ligand-binding isotherm and the concentration of $\mathscr{P}\mathscr{L}_i$ are given by [2]

$$\nu^{\beta} = \frac{nkC^{\beta}_{\mathscr{L}}}{1 + kC^{\beta}_{\mathscr{L}}} \tag{5}$$

and

$$C^{\beta}_{\mathscr{P}\mathscr{L}_i} = \frac{\bar{C}^{\beta}_{\mathscr{P}}\binom{n}{i}(kC^{\beta}_{\mathscr{L}})^{i}}{(1 + kC^{\beta}_{\mathscr{L}})^{n}} \tag{6}$$

Substituting eqs. 3, 5 and 6 into eq. 4 gives

$$\nu_{ss} = \frac{nkC^{\beta}_{\mathscr{L}}}{1 + kC^{\beta}_{\mathscr{L}}} - \sum_{i=1}^{n} i\frac{(V_{\mathscr{P}\mathscr{L}_i} - \bar{V}_{\mathscr{P}})}{(V_{\mathscr{L}} - \bar{V}_{\mathscr{P}})} \cdot \frac{\binom{n}{i}(kC^{\beta}_{\mathscr{L}})^{i}}{(1 + kC^{\beta}_{\mathscr{L}})^{n}} \tag{7}$$

Since ν_{ss} is an implicit function of protein concentration through $C^{\beta}_{\mathscr{L}}$, extrapolation to infinite dilution of protein is indicated. Eq. 3 tells us that $C^{\beta}_{\mathscr{L}} \to C^{\alpha}_{\mathscr{L}}$ as $\bar{C}^{\beta}_{\mathscr{P}} \to 0$. In this limit

$$\bar{V}_{\mathscr{P}} = \left[V_{\mathscr{P}} + \sum_{i=1}^{n}\binom{n}{i}(kC^{\alpha}_{\mathscr{L}})^{i}V_{\mathscr{P}\mathscr{L}_i}\right]/(1 + kC^{\alpha}_{\mathscr{L}})^{n} \tag{8}$$

By substituting $C^{\alpha}_{\mathscr{L}}$ for $C^{\beta}_{\mathscr{L}}$ and eq. 8 for $\bar{V}_{\mathscr{P}}$ in eq. 7 and recalling that operationally the steady-state binding constant, k_{ss}, is given by

$$k_{ss} = [\nu_{ss}/(n - \nu_{ss})]/C^{\alpha}_{\mathscr{L}} \tag{9}$$

it is found that at infinite dilution (designated by superscript ∞)

$$\nu^{\infty}_{ss} = \frac{nk^{\infty}_{ss}C^{\alpha}_{\mathscr{L}}}{1 + k^{\infty}_{ss}C^{\alpha}_{\mathscr{L}}} \tag{10}$$

where

$$k^{\infty}_{ss} = \frac{k(A - B)}{A + kC^{\alpha}_{\mathscr{L}}B} \tag{11}$$

in which

$$A = n(1 + kC^{\alpha}_{\mathscr{L}})^{n-1}\sum_{j=0}^{n}(V_{\mathscr{L}} - V_{\mathscr{P}\mathscr{L}_j})\binom{n}{j}(kC^{\alpha}_{\mathscr{L}})^{j}$$

$$B = \sum_{i=1}^{n} i\left[\sum_{j=0}^{n}(V_{\mathscr{P}\mathscr{L}_i} - V_{\mathscr{P}\mathscr{L}_j})\binom{n}{j}(kC^{\alpha}_{\mathscr{L}})^{j}\right] \times\left[\binom{n}{i}(kC^{\alpha}_{\mathscr{L}})^{i-1}\right] \tag{12}$$

We now introduce the assumptions that: (1) the binding of ligand, while changing the net charge on the protein, has a negligible effect on its frictional coefficient; and (2) each ligand molecule bound increases the electrophoretic velocity of its complex by the same amount, w. Under these assumptions [4]

$$V_{\mathscr{P}\mathscr{L}_i} = V_{\mathscr{P}} + iw \tag{13}$$

in which case eq. 11 reduces to

$$k^{\infty}_{ss} = \left(\frac{(V_{\mathscr{L}} - V_{\mathscr{P}}) - \dfrac{(1 + nkC^{\alpha}_{\mathscr{L}})w}{(1 + kC^{\alpha}_{\mathscr{L}})}}{(V_{\mathscr{L}} - V_{\mathscr{P}}) - \dfrac{(n-1)kC^{\alpha}_{\mathscr{L}}w}{(1 + kC^{\alpha}_{\mathscr{L}})}}\right)k \tag{14}$$

For $n = 1$

$$k^{\infty}_{ss} = \left(\frac{V_{\mathscr{L}} - V_{\mathscr{P}\mathscr{L}}}{V_{\mathscr{L}} - V_{\mathscr{P}}}\right)k \tag{15}$$

and the double-reciprocal plot of ν^{∞}_{ss} vs. $C^{\alpha}_{\mathscr{L}}$ is linear. It is evident that for $n \geq 2$ the double-reciprocal plot is virtually linear, and k^{∞}_{ss} can be

approximated by its value at $kC^{\alpha}_{\mathscr{L}} = 1$

$$k^{\infty}_{ss} = \left(\frac{2(V_{\mathscr{L}} - V_{\mathscr{P}}) - (n+1)w}{2(V_{\mathscr{L}} - V_{\mathscr{P}}) - (n-1)w}\right)k \tag{16}$$

which introduces an error of only 0.1–0.3% depending upon the value of n.

The conclusion reached is that extrapolation of steady-state binding constants to infinite dilution of protein does not yield the intrinsic binding constant directly, rather the product of a kinetic factor and the equilibrium constant.

Finally, it can also be concluded from eq. 3 that the larger the value of k or n, the greater the difference between $C^{\beta}_{\mathscr{L}}$ and $C^{\alpha}_{\mathscr{L}}$ and, thus, the greater the deviation of k_{ss} from k. This can be seen as follows: Substituting eq. 6, eq. 8 with $C^{\beta}_{\mathscr{L}}$ replacing $C^{\alpha}_{\mathscr{L}}$, and eq. 13 into eq. 3, evaluating the sums, and solving the resulting quadratic equation for $C^{\beta}_{\mathscr{L}} - C^{\alpha}_{\mathscr{L}}$ at the midpoint value, $kC^{\alpha}_{\mathscr{L}} = 1$, and fixed $\bar{C}^{\beta}_{\mathscr{P}}$ gives

$$C^{\beta}_{\mathscr{L}} - C^{\alpha}_{\mathscr{L}} = \left(\tfrac{1}{2}\right)\left[-b + (b^2 - 4c)^{\frac{1}{2}}\right]$$

$$b = \frac{\left[2(V_{\mathscr{L}} - V_{\mathscr{P}}) - nw + n\bar{C}^{\beta}_{\mathscr{P}}wk\right]}{\left[(V_{\mathscr{L}} - V_{\mathscr{P}}) - nw\right]k} \tag{17}$$

$$c = \frac{n\bar{C}^{\beta}_{\mathscr{P}}w}{\left[(V_{\mathscr{L}} - V_{\mathscr{P}}) - nw\right]k}$$

Normalized values, $(C^{\beta}_{\mathscr{L}} - C^{\alpha}_{\mathscr{L}})/C^{\alpha}_{\mathscr{L}}$, were compared for the assignments: $V_{\mathscr{L}} = 8 \times 10^{-4}$ cm s^{-1}, $V_{\mathscr{P}} = -1.6 \times 10^{-4}$, $w = 0.4 \times 10^{-4}$ cm s^{-1} (mol ligand bound)$^{-1}$, and $\bar{C}^{\beta}_{\mathscr{P}} = 1 \times 10^{-5}$ M. Thus, for example, for $n = 1$ and $k = 5 \times 10^4$ M^{-1}, $(C^{\beta}_{\mathscr{L}} - C^{\alpha}_{\mathscr{L}})/C^{\alpha}_{\mathscr{L}} = -0.010$; for $k = 5 \times 10^6$ M, -0.601. For $k = 5 \times 10^5$ M^{-1} and $n = 1$, $(C^{\beta}_{\mathscr{L}} - C^{\alpha}_{\mathscr{L}})/C^{\alpha}_{\mathscr{L}} = -0.100$; $n = 4$, -0.351.

In order to appreciate fully the practical implications of the foregoing formulation, they were evaluated numerically as described below.

2.2. Numerical transport calculations

Most of the calculations are for the reaction

$$\mathscr{P} + \mathscr{L} \rightleftharpoons \mathscr{P}\mathscr{L}, k \tag{18}$$

in which the negatively charged protein binds a single cationic ligand molecule, but statistical binding to two equivalent sites on the protein molecule

$$\begin{aligned} &\mathscr{P} + \mathscr{L} \rightleftharpoons \mathscr{P}\mathscr{L}, && 2k \\ &\mathscr{P}\mathscr{L} + \mathscr{L} \rightleftharpoons \mathscr{P}\mathscr{L}_2, && \left(\tfrac{1}{2}\right)k \end{aligned} \tag{19}$$

was also considered. In both cases, binding of ligand causes a change in the electrophoretic mobility but not the frictional coefficient of the protein. Counterion electrophoretic patterns were computed by numerical solution of the appropriate set of transport equations and mass actions expressions. Since the form of the equations and the numerical procedures are detailed elsewhere for several illustrative, rapidly equilibrating systems [5–9], only a brief description is warranted here: (1) Both diffusional and driven transport were assumed to be ideal; i.e., diffusion coefficients, D, electrophoretic mobilities, μ, and electric field strength, E, invariant through the electrophoresis column. (2) The implicit Crank-Nicholson method [5,7,10] was used to approximate the partial differential transport equations by finite-difference equations, correction being made for the major fraction of the truncation error due to the way the first spatial derivative is approximated [5,6,8,11]. (3) The difference equations were solved in a static coordinate system, $\Delta x = 0.0025$ cm and $\Delta t = 10$ s, with initial and boundary conditions simulating experimental procedure. (4) Initial conditions: A thin, 0.025 cm, uniform zone of $\mathscr{P}$ at loading concentration $C^{o}_{\mathscr{P}}$ centered 0.3 cm from the cathodic end of the electrophoresis column, and $\mathscr{L}$ at concentration $C^{\alpha}_{\mathscr{L}}$ in the last segment at the anodic end representing the interface between the column and the ligand-containing electrode compartment. (5) Boundary conditions: For $\mathscr{P}$ and $\mathscr{P}\mathscr{L}_i$, a sink at both ends of the column; for $\mathscr{L}$, a source of concentration $C^{\alpha}_{\mathscr{L}}$ at the anodic end of the column and a sink at the cathodic end; i.e., infinitely large electrode compartments. (6) After each time cycle of transport, chemical equilibrium was recalculated by applying the appropriate mass action expressions. (7) The overall time of electrophoresis was sufficient to attain the steady state as judged by the criterion that the value of $C_{\mathscr{L}}$ over a reasonable span upstream from the migrating zone of protein (figs. 2 and 3) should equal $C^{\alpha}_{\mathscr{L}}$ to within

99.5%. When this criterion was satisfied, the value of $C_{\mathscr{L}}$ at the minimum of the trough of unbound ligand coincident with the migrating zone of protein (figs. 2 and 3) agreed to within 99.9% with $C^{\beta}_{\mathscr{L}}$ calculated from eq. 3.

ν_{ss} was calculated according to its operational definition

$$\nu_{ss} = \frac{\sum_{j=a}^{b}\left(\sum_{i=1}^{n} iC_{\mathscr{P}\mathscr{L}_i}(j) + C_{\mathscr{L}}(j) - C^{\alpha}_{\mathscr{L}}\right)}{\sum_{j=a}^{b}\sum_{i=0}^{n} C_{\mathscr{P}\mathscr{L}_i}(j)} \qquad (20)$$

where j is the segment number, the sum over the protein zone being taken between limits a and b at which positions $\bar{C}_{\mathscr{P}}$ was usually three or more orders of magnitude (in three cases two orders of magnitude) less than at the apex. We define the apparent number of moles of ligand bound per mole of protein (apparent in the sense that the local $C_{\mathscr{L}} \neq C^{\alpha}_{\mathscr{L}}$) as

$$\nu_{app} = \frac{\sum_{j=a}^{b}\sum_{i=1}^{n} iC_{\mathscr{P}\mathscr{L}_i}(j)}{\sum_{j=a}^{b}\sum_{i=0}^{n} C_{\mathscr{P}\mathscr{L}_i}(j)} \qquad (21)$$

Most of the calculations are for the midpoint value, $kC^{\alpha}_{\mathscr{L}} = 1$; and k_{ss} and the apparent binding constant, k_{app}, were obtained respectively from eq. 9 and the analogous equation in which ν_{app} replaces ν_{ss}. The results of other calculations were used to construct double-reciprocal plots of ν_{ss} vs. $C^{\alpha}_{\mathscr{L}}$. A range of values for the parameters, $C^{o}_{\mathscr{P}}$ and k, was explored.

Transport parameters were assigned the following values: Unless indicated otherwise, $D_{\mathscr{P}} = D_{\mathscr{P}\mathscr{L}} = 2.1 \times 10^{-7}$ cm^2 s^{-1}; $\mu_{\mathscr{P}} = -4 \times 10^{-5}$ cm^2 s^{-1} V^{-1}, $\mu_{\mathscr{P}\mathscr{L}} = -3 \times 10^{-5}$ and $\mu_{\mathscr{P}\mathscr{L}_2} = -2 \times 10^{-5}$; $E = 4$ V cm^{-1}, $V = \mu E$ so that $w = 0.4 \times 10^{-4}$ cm s^{-1} (mol ligand bound)$^{-1}$; $D_{\mathscr{L}} = 1.0 \times 10^{-5}$ and $\mu_{\mathscr{L}} = 2 \times 10^{-4}$.

Computations were made on the University of Colorado's Cyber 172 electronic computer. Control calculations showed that the uncoupled species migrated and diffused accurately. Material balance was excellent in all cases, the electrophoresis column being sufficiently long, 4.5 cm, that an insignificant amount of protein was lost to the sinks at either end of the column. The time of electrophoresis required to attain the steady state was 2.25×10^4 s for all conditions considered below.

Theoretical steady-state patterns are displayed as plots of $\bar{C}_{\mathscr{P}}$ and $C_{\mathscr{L}}$ vs. position, x, in the electrophoresis column. The vertical arrows labeled $\mathscr{P}$ and $\mathscr{P}\mathscr{L}$ at the top of the figures indicate where the peaks in the pattern would have been located had electrophoresis been carried out on a mixture of two noninteracting proteins having the same electrophoretic mobilities as $\mathscr{P}$ and $\mathscr{P}\mathscr{L}$.

3. Results

Representative steady-state counterion electrophoretic patterns calculated numerically for reaction 18 are displayed in figs. 2 and 3. It is immediately apparent that the patterns are in accord

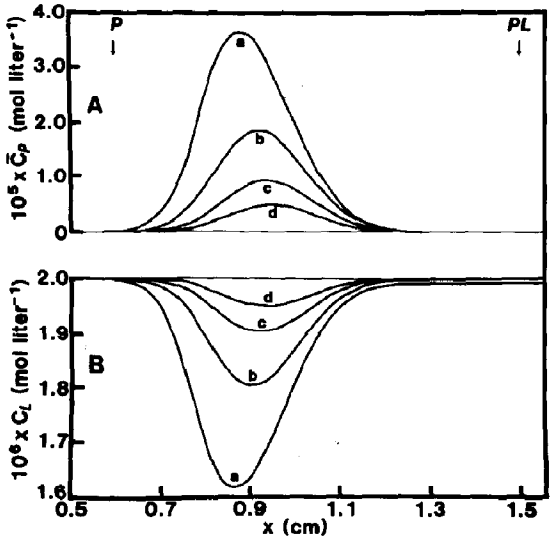

Fig. 2. Effect of protein concentration on the steady-state counterion electrophoretic patterns computed for reaction 18, $k = 5 \times 10^5$ M^{-1} and $kC^{\alpha}_{\mathscr{L}} = 1$: (a) $C^{o}_{\mathscr{P}} = 3.24 \times 10^{-4}$ M, (b) 1.62×10^{-4} M, (c) 8×10^{-5}, (d) 4×10^{-5}. In this figure and figs. 3 and 7, A is the protein pattern and B the concentration profile of unbound ligand; migration of protein is from right to left with ligand being driven to the right; time of electrophoresis, 2.25×10^4 s.

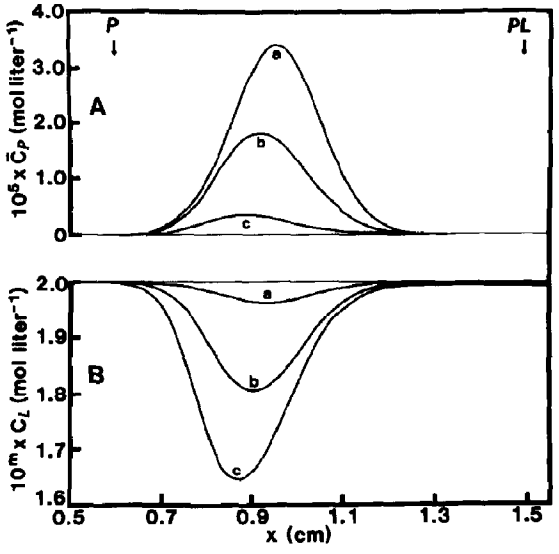

Fig. 3. Effect of intrinsic ligand-binding constant on the steady-state counterion electrophoretic patterns computed for reaction 18, $kC^o_{\mathscr{L}} = 1$ and $C^o_{\mathscr{P}}$ graded so as to scale the unbound ligand-concentration profiles: (a) $k = 5 \times 10^4$ M^{-1}, $m = 4$, $C^o_{\mathscr{P}} = 3 \times 10^{-4}$ M; (b) $k = 5 \times 10^5$ M^{-1}, $m = 5$, $C^o_{\mathscr{P}} = 1.62 \times 10^{-4}$ M; (c) $k = 5 \times 10^6$ M^{-1}, $m = 6$, $C^o_{\mathscr{P}} = 3 \times 10^{-5}$ M.

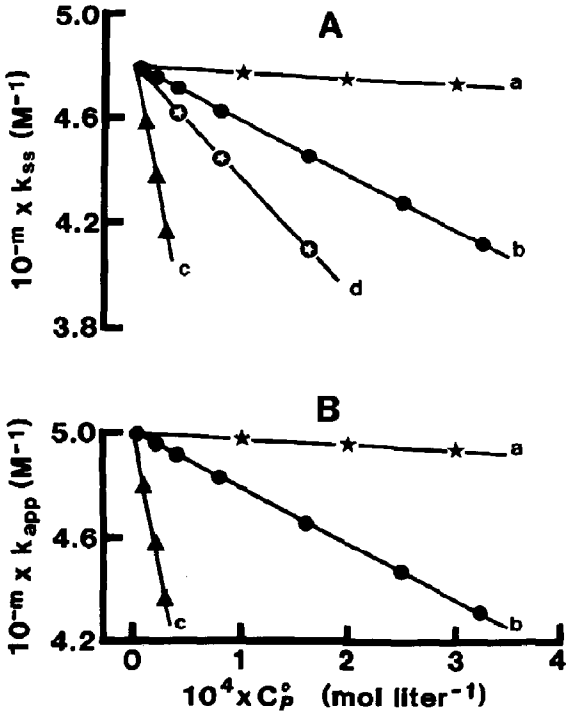

Fig. 4. Steady-state binding constants (A) and apparent binding constants (B) calculated from theoretical steady-state counterion electrophoretic patterns for reaction 18. Effect of the magnitude of the intrinsic binding constant on the discrepancy between these quantities and the intrinsic constant at a given protein concentration, and extrapolation to infinite dilution of protein: (a) $k = 5 \times 10^4$ M^{-1}, $m = 4$; (b) $k = 5 \times 10^5$ M^{-1}, $m = 5$; (c) $k = 5 \times 10^6$ M^{-1}, $m = 6$. The data points in a, b and c were calculated for the midpoint value $kC^o_{\mathscr{L}} = 1$; d corresponds to b in that $k = 5 \times 10^5$ M^{-1}, but the data points were derived from double-reciprocal plots of ν_{ss} vs. $C^o_{\mathscr{L}}$.

with the predictions of eqs. 3 and 17. Thus, there is a trough in the concentration profile of unbound ligand, the trough migrating coincidentally with the zone of protein. Moreover, the depth of the trough decreases with decreasing protein concentration (fig. 2) and is sensitive to the magnitude of the intrinsic ligand-binding constant, increasing markedly with increasing k (fig. 3). As anticipated these properties are reflected in the values of the steady-state binding constant and the apparent binding constant derived from the patterns. The plots of k_{ss} and k_{app} vs. $C^o_{\mathscr{P}}$ presented in fig. 4 for a 100-fold range of k values illustrate this point.

Extrapolation of k_{ss} to infinite dilution of protein (fig. 4A) gives a value for k^∞_{ss} ($= 4.79 \times 10^m$ M^{-1} for $k = 5 \times 10^m$ M^{-1}, $m = 4, 5, 6$) equal to the value (4.7917×10^m M^{-1}) predicted by eq. 15. This result was confirmed by calculations made for $k = 5 \times 10^5$ M^{-1} at the extremely low concentration of $C^o_{\mathscr{P}} = 1.25 \times 10^{-9}$ M, which gave $k_{ss} = 4.7917 \times 10^5$ M^{-1} independent of the half-width of the protein zone ($= 0.10$ or 0.16 cm at $\bar{C}_{\mathscr{P}} =$ $\bar{C}_{\mathscr{P},apex} e^{-0.5}$ for $D_{\mathscr{P}} = 2.1 \times 10^{-7}$ or 6.0×10^{-7} cm^2 s^{-1} at constant $t = 2.25 \times 10^4$ s). This close agreement between the numerical results and the analytical prediction, based on certain conditions specified early on, could be interpreted to mean that the diffusing protein zone is still sufficiently narrow so as to approximate an infinitely sharp one. On the other hand, a more plausible explanation may reside in the observation that the distributions of $\mathscr{P}$, $\mathscr{PL}$ and $(C_{\mathscr{L}} - C^a_{\mathscr{L}})$ have about the same positions and half-widths even at rather high protein concentrations. Moreover, except for the

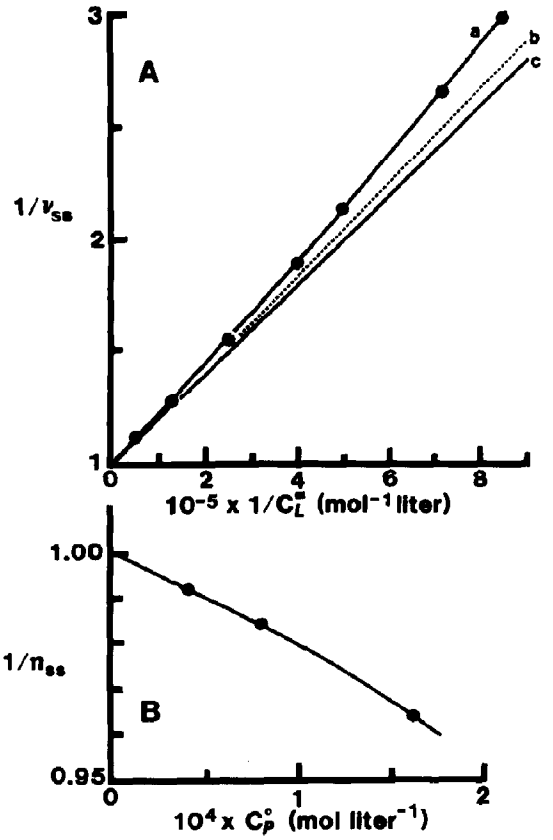

Fig. 5. Simulation of counterion electrohoretic experiments. A: (a) double-reciprocal plot of ν_{ss} vs. $C_{\mathscr{P}}^o$, each data point derived from a steady-state pattern computed for reaction 18, $k = 5 \times 10^5$ M^{-1} and $C_{\mathscr{P}}^o = 1.62 \times 10^{-4}$ M; (b) diagrammatic plot for the limit of infinite dilutions of protein, $k_{ss}^{\infty} = 4.7917 \times 10^5$ M^{-1} as given by eq. 15; (c) diagrammatic plot for equilibrium dialysis experiments, $k = 5 \times 10^5$ M^{-1}, in which the equilibrium concentration of unbound ligand equals $C_{\mathscr{L}}^a$. B: steady-state number of binding sites on the protein molecule (reaction 18) derived from double-reciprocal plots calculated for decreasing protein concentration, extrapolation to infinite dilution.

position of $\mathscr{L}$, these respective properties converge to the same values as the protein concentration is lowered: At $C_{\mathscr{P}}^o = 3.24 \times 10^{-4}$ M the position of the apex and the half-width for $\mathscr{P}$ are 0.8775 and 0.09625 cm, respectively; for $\mathscr{P}\mathscr{L}$, 0.8800 and 0.1050 cm; for $\mathscr{L}$, 0.8650 and 0.1025 cm. At $C_{\mathscr{P}}^o = 1.25 \times 10^{-6}$ and 1.25×10^{-9} M: for both $\mathscr{P}$ and $\mathscr{P}\mathscr{L}$, 0.9625 and 0.0975 cm; for $\mathscr{L}$, 0.9475 and 0.0975 cm. Although the position of the distribution of $(C_{\mathscr{L}} - C_{\mathscr{L}}^a)$ does not converge to that of $\mathscr{P}$ and $\mathscr{P}\mathscr{L}$, the difference is only 0.015 cm. Whichever explanation pertains, these results lend confidence in the application of eq. 15 (and as we shall see shortly, eq. 16) to experimental situations, particularly since sharp zones are a characteristic feature of disc electrophoresis.

In contrast to k_{ss}, k_{app} extrapolates to k at infinite dilution (fig. 4B). Thus, if a method can be devised to analyze selectively for the amount of bound ligand in the protein zone, k can be determined directly by extrapolation.

The data points defining lines a, b and c in fig. 4 were determined at the midpoint value of $kC_{\mathscr{L}}^a = 1$, but values of k_{ss} have also been derived from double-reciprocal plots of ν_{ss} vs. $C_{\mathscr{P}}^a$. As anticipated, the plots are curvilinear at finite protein concentration (fig. 5A) but in practice one might be led to fit such data to a straight line. Accordingly, we have fitted our data points by linear least squares and have calculated values for n_{ss} and k_{ss} from the intercept and slope. The resulting values of k_{ss} are understandably smaller than those determined at the midpoint, but as shown by line d in fig. 4A they too extrapolate to the value of k_{ss}^{∞}

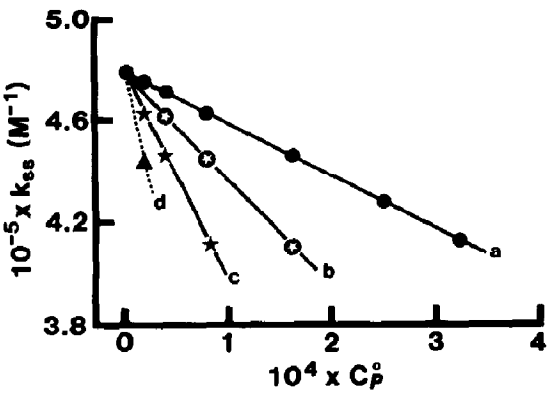

Fig. 6. Comparison of steady-state binding constants calculated for $n = 1$ (reaction 18) and $n = 2$ (reaction 19), $k = 5 \times 10^5$ M^{-1}. Effect of n on the discrepancy between the steady-state and intrinsic constant, and extrapolation to infinite dilution: (a) $n = 1$ with data points calculated for $kC_{\mathscr{L}}^a = 1$, (b) $n = 1$ with data points derived from double-reciprocal plots of ν_{ss} vs. $C_{\mathscr{P}}^o$, (c) $n = 2$ with data point calculated for $kC_{\mathscr{L}}^a = 1$, (d) $n = 2$ with data point derived from double-reciprocal plot.

predicted by eq. 15. As expected, linearization of the double-reciprocal plot slightly underestimates n_{ss}, but extrapolation to infinite dilution gives the stoichiometric value (fig. 5B).

The foregoing calculations were extended to include statistical binding to two sites on the protein molecule (reaction 19). The shape of the resulting steady-state patterns were quite similar to that for $n = 1$ (reaction 18) with one exception: as anticipated from eq. 17, the depth of the trough in the concentration profile of unbound ligand was much greater for the same $k = 5 \times 10^5$ M^{-1}, $C_{\mathscr{P}}^{o}$ and t. Values of k_{ss} calculated for the two systems are compared in fig. 6. Two conclusions emerge. First, the discrepancy between k_{ss} and k is considerably greater for $n = 2$ than for $n = 1$, and according to eq. 17 the discrepancy would increase continuously with further increase in n. Second, extrapolation of k_{ss} for $n = 2$ to infinite dilution of protein gives the value, 4.79×10^5 M^{-1}, for k_{ss}^{∞} which agrees with the value, 4.7872×10^5 M^{-1}, predicted by eq. 16.

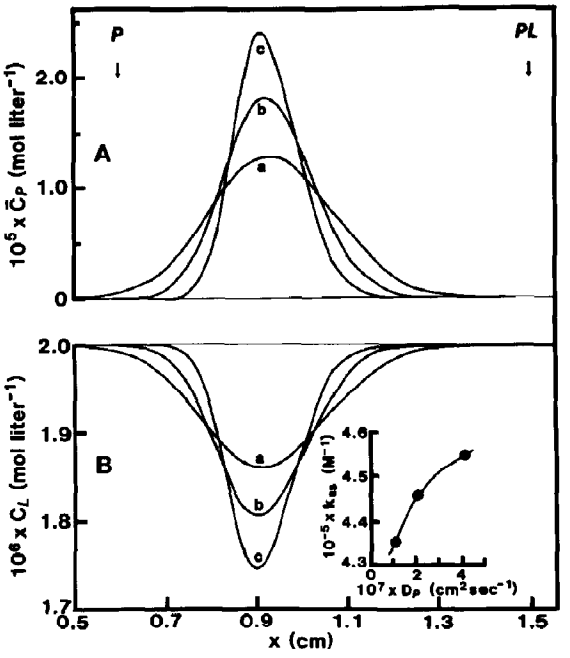

Fig. 7. Effect of the diffusion coefficient of the protein on the steady-state counterion electrophoretic patterns computed for reaction 18 with $k = 5 \times 10^5$ M^{-1}, $kC_{\mathscr{L}}^{a} = 1$ and $C_{\mathscr{P}}^{o} = 1.62 \times 10^{-4}$ M: (a) $D_{\mathscr{P}} = 4.20 \times 10^{-7}$ cm^2 s^{-1}, (b) 2.10×10^{-7}, (c)1.05×10^{-7}. Inset: effect of diffusion coefficient on the steady-state binding constant k_{ss}.

To round out our calculations we have explored the effect of diffusion on the steady-state pattern and the value of k_{ss}. As shown in fig. 7, the smaller the diffusion coefficient of the protein, all else held constant, the sharper is the zone of protein and, thus, the deeper the trough in the concentration profile of unbound ligand. Consequently, the greater is the discrepancy between k_{ss} and k (fig. 7 inset).

4. Discussion

Practical assessment of the results presented above requires consideration of the load of protein applied to the electrophoresis column. For a cylindrical gel column 0.6 cm in diameter and an initial zone 0.025 cm thick the load is $7.07 C_{\mathscr{P}}^{o} M$ μg, where M is the molecular mass of the protein. In the calculations for $n = 2$ and $k = 5 \times 10^5$ M^{-1} (lines c and d in fig. 6) the maximum loading concentration considered was $C_{\mathscr{P}}^{o} = 8 \times 10^{-5}$ M which, for $M = 5 \times 10^4$ Da, corresponds to a load of 28 μg. This is to be compared with the load of 150–200 μg used in the experiments on intestinal calcium-binding protein [1], $M \simeq 1 \times 10^4$ Da and two calcium-binding sites with an apparent binding constant of about 10^6 M^{-1}. Referring back to fig. 6, it is clear that, as practiced, the discrepancy between k_{ss} and k would be unacceptable; conceivably the difference could be, perhaps, as much as an order of magnitude. Accordingly, k_{ss} must be extrapolated to infinite dilution of protein, and k evaluated from k_{ss}^{∞} using eq. 15 or 16.

The burden of data acquisition can be lightened by constructing a single double-reciprocal plot of ν_{ss} vs. $C_{\mathscr{L}}^{a}$ to estimate n and to guide the extrapolation of k_{ss} values determined at a fixed $C_{\mathscr{L}}^{a}$ close to the midpoint of the titration. (Note that the extrapolation will most likely be linear only at low protein concentrations.) The kinetic factor in eqs. 15 and 16 is evaluated from the results of independent experiments designed to determine the several electrophoretic velocities (note that $w = (V_{\mathscr{P}\mathscr{L}_n} - V_{\mathscr{P}})/n$). Although the value of the kinetic factor

for the particular parameter assignments made in our calculations was close to unity (≈ 0.96) it could be as small as 0.5 depending upon electrophoretic velocities.

Experimental application of eqs. 15 and 16 is actually an approximation, since they were derived assuming ideal electrophoresis while disc electrophoresis is nonideal, the conductance and pH changing across the zone of protein [12,13]. Although k_{ss} is extrapolated to infinite dilution, the value of k_{ss}^{∞} can be expected to differ from the true value, because the gradients of conductance and pH do not approach zero asymptotically as the concentration of protein is decreased [14]. However, in a related vein, the apparent composition of a mixture of proteins determined from moving-boundary electrophoretic patterns is also subject to these effects but extrapolates to a value only slightly different from the true composition [14]. This leads us to believe that the experimental k_{ss}^{∞} likewise will differ only slightly from its true value and that the proposed procedure for determining k is valid.

Finally, it is instructive to examine the consequences of conservation of mass as expressed by eq. 3 for isoelectric focusing and molecular sieve chromatography. In the case of isoelectric focusing the effect of a charged ligand on the isoelectric point of a protein can be used to determine the intrinsic binding constant [9]. In essence, the method relies on analysis of steady-state patterns attained in much the same way as in counterion electrophoresis, the fundamental difference being that in isoelectric focusing $\bar{V}_{\mathscr{P}} = 0$. Since $V_{\mathscr{P}\mathscr{L}_i} \neq 0$, eq. 3 tells us that there will still be a trough in the concentration profile of unbound ligand, so that the steady-state binding constant must be extrapolated to infinite dilution [9]. In contrast, the Hummel-Dreyer gel chromatographic method [15] is free from this complication, because both uncomplexed and complexed protein are excluded from Sephadex G-25 as they move down the column in the mobile phase. In other words, $V_{\mathscr{P}\mathscr{L}_i} = \bar{V}_{\mathscr{P}}$ and eq. 3 tells us that $C_{\mathscr{L}}^{\beta} = C_{\mathscr{L}}^{\alpha}$.

Acknowledgement

This work was supported in part by Research Grant GM 28793 from the National Institutes of General Medical Sciences, National Institutes of Health, U.S. Public Health Services.

References

1 T.-H. Ueng and F. Bronner, Arch. Biochem. Biophys. 197 (1979) 205.
2 I.M. Klotz, in: The proteins, vol. 1, part B, 1st edn., eds. H Neurath and K. Bailey (Academic Press, New York, 1953) ch. 8.
3 R.A. Alberty and H.H. Marvin, Jr, J. Phys. Colloid Chem. 54 (1950) 47.
4 R.F. Smith and D.R. Briggs, J. Phys. Colloid Chem. 54 (1950) 33.
5 W.B. Goad, in: Interacting macromolecules. The theory and practice of their electrophoresis, ultracentrifugation, and chromatography, ed. J.R. Cann (Academic Press, New York, 1970) ch. 5.
6 J.R. Cann and G. Kegeles, Biochemistry 13 (1974) 1868.
7 J.R. Cann and N.D. Hinman, Biochemistry 15 (1976) 4614.
8 J.R. Cann and D.I. Stimpson, Biophys. Chem. 7 (1977) 103.
9 J.R. Cann and K.J. Gardiner, Biophys. Chem. 10 (1979) 211.
10 B. Carnahan, H.A. Luther and J.O. Wilkes, Applied numerical methods (John Wiley and Sons, New York, 1969) p. 440.
11 W.B. Goad and J.R. Cann, Ann. N.Y. Acad. Sci. 164 (1969) 172.
12 L. Ornstein, Ann. N.Y. Acad. Sci. 121 (1964) 321.
13 M. Bier, O.A. Palusinski, R.A. Mosher and D.A. Saville, Science 219 (1983) 1281.
14 L.G. Longsworth, in: Electrophoresis theory, methods and applications, vol. 1, ed. M. Bier (Academic Press, New York, 1959) ch. 3, p. 113.
15 J.P. Hummel and W.J. Dreyer, Biochim. Biophys. Acta 63 (1962) 530.